

## **EFFECTS OF THE H-BOND BRIDGE GEOMETRY ON THE VIBRATIONAL SPECTRA OF WATER: THE SIMPLEST MODELS OF THE H-BOND POTENTIAL**

**Yu. Ya. Efimov**

UDC 532.74

The approach suggested in this work within the fluctuation theory of the hydrogen bond allows one to correlate the vibrational band shape with the statistical distribution of the geometrical parameters of the O–H...O hydrogen bridge, generated by the local fluctuations of the molecular surroundings in liquids. The correlation may be established either exclusively from spectral data or by also using the known empirical correlations with structural data. The existing explanations to the anomalous broadening of the spectral bands of associated liquids, namely, the dominant effect of the  $R_{O...O}$  bond length or the  $\varphi(H-O...O)$  bending angle on the OH vibration frequency were tested. Both hypotheses provided an adequate description of the experimental spectra and their temperature dependence. However, the required relationship between the frequency and geometrical parameters conflicts with several empirical facts, indicating that the one-parameter potentials are insufficient for a quantitative description of H-bonds in liquids. A method for the design and verification of more complex potentials containing all geometrical parameters of the hydrogen bridge affecting the H-bond energy is suggested.

**Keywords:** liquid water, continuum model, hydrogen bond, fluctuation theory, geometry, potential, vibrational spectra.

### **INTRODUCTION**

The problem of the structure of liquid water and interpretation of its vibrational spectra has a century-long history and is discussed in thousands of publications (see review [1]). Today two groups of water structure models are dominant. The mixture model was suggested by Roentgen [2]; its various modifications represent water as a mixture of associates (monomers, dimers, small clusters, etc.). Broken hydrogen bonds are essential attributes of the model (see, e.g., [3, 4]). In the continuum model, water is interpreted as a “polymer” whose structure fluctuates in time. It is determined by a continuous three-dimensional network of hydrogen bonds that differ in their geometrical parameters, energy, and vibration frequencies of the involved oscillators. This model was suggested by Bernal and Fowler [5], as well as Langmuir, who compared an ocean to a macromolecule. The history and detailed discussion of this model are found, e.g., in [6, 7].

The mathematical formulation of the mixture model is much simpler and therefore more popular with chemists and experimenters. Thus, the work of an international research group using this model [9] was included among the first ten scientific achievements of 2004 [8]. The main conclusion of their work was that half of all hydrogen bonds were broken and

---

Institute of Chemical Kinetics and Combustion, Siberian Division, Russian Academy of Sciences, Novosibirsk; efimov@kinetics.nsc.ru. Translated from *Zhurnal Strukturnoi Khimii*, Vol. 49, No. 2, pp. 275-283, March-April, 2008. Original article submitted June 15, 2007.

cleavage continued at elevated temperatures; however, this conflicts with a number of reliable experimental facts and the results of computer simulations. In particular, this is inconsistent with the spectrum shape and its temperature dependence. The correct results of the experiment (decreased mean energy of hydrogen bonds per molecule at elevated temperatures) were incorrectly interpreted as cleavage of some part of hydrogen bonds, caused by heating and leaving other bonds as strong as they were in ice. The canonical mixture model precludes an alternative explanation because heating should lead to a redistribution of the concentrations of objects of different sorts with fixed properties.

The continuum model qualitatively explains these results by the weakening of all H-bonds of water that form a single statistical ensemble, rather than by cleavage of some part of H-bonds. Moreover, the theory based on the continuum model allowed researchers to *quantitatively* describe the form of the experimental Raman [10, 11] and IR absorption spectra [12, 13] in the range from 0°C to 200°C, to explain their absolutely different behaviors, and to calculate the contributions of hydrogen bonds to the major thermodynamic functions [14]. This is a purely static theory; it does not consider the dynamics of a molecular assembly in time. However, the adequacy of the static approximation was confirmed by the integrated innovative studies by molecular dynamics, quantum-chemical, and femtosecond laser spectroscopy methods [15, 16]. It appeared that the static contours were the basis of the anomalously wide bands in the spectra of water [15], while the dynamic effects (spectral diffusion, which is well known in NMR [17] but was not previously discussed in optics) merely modified their form [15, 16]. Regretfully, the calculations reported in these works are now possible for very small molecular assemblies (of the order of a hundred molecules) and demand very large computer resources (thousands of hours of processor time). At the same time, theoretical analysis of the re-recorded Raman spectra of water unambiguously points to a continuous statistical energy distribution of the quasitetrahedrally coordinated (authors' terminology) hydrogen bonds of its molecules [18]. All this stimulates further elaboration of the continuum model in its static version by establishing the relationship between the geometrical, energy, and spectroscopic characteristics of hydrogen bonds in water. This work seeks an accurate solution to the problem of this relationship to describe the temperature evolution of the experimental spectra in terms of the statistics of the geometrical parameters of hydrogen bonds based on the two simple explanations of the wide distribution of the vibration frequencies of water. The problem is solved within the framework of the pure spectroscopic approach and the approach that also uses the available data about correlation between the OH vibration frequency and the hydrogen bridge geometry.

## H-BOND ENERGY STATISTICS AND ITS EFFECTS ON THE SPECTRAL CONTOUR SHAPE

According to A. P. Zhukovskii's algorithm [19] that implements the fluctuation theory of the hydrogen bond in spectroscopy, the statistical distribution of the OH vibration frequencies of water molecules at any temperature  $T$  is considered Boltzmann's distribution,

$$P(\nu, T) = Q^{-1}(T)W(\nu)\exp[-E(\nu)/(k_B T)] \quad (1)$$

and is determined by both the energy of the particular H bond  $E(\nu)$  and its degeneracy  $W(\nu)$ . Here  $Q(T)$  is the statistical integral in its conventional form (used in (1) to normalize the area distribution  $P(\nu, T)$  to unity); and  $k_B$  is Boltzmann's constant. It follows that the frequency  $\nu_{OH}$  is the sole parameter used to express all other parameters. It is interesting that in recent works [16, 18, 20], using various methods (quantum-chemical optimization, structural analysis of many molecular dynamic models) also led to the conclusion that  $\nu_{OH}$  depends on a single quantity, namely, the projection of the electric field on the direction of the OH group at the proton site. Thus, two different approaches to spectrum interpretation revealed a single parameter (the energy of a particular hydrogen bond or the strength of an electric field induced on it by its neighbors), which determines the OH vibration frequency.

It was shown [11, 21] that the three functions of (1) could be calculated from the vibrational spectra of semideuterated water HOD molecules at several temperatures (Fig. 1b: the energy is given in kJ/mol; the doubled  $W(\nu)$  logarithm, in dimensionless units). The spectra reconstructed from them with the use of (1) describe the experiment over the whole temperature range and do this better than any other of the available theories (Fig. 1a). The mechanism of the formation of the spectral contour is illustrated by Fig. 1c; the statistic frequency distribution is the product of the temperature-independent

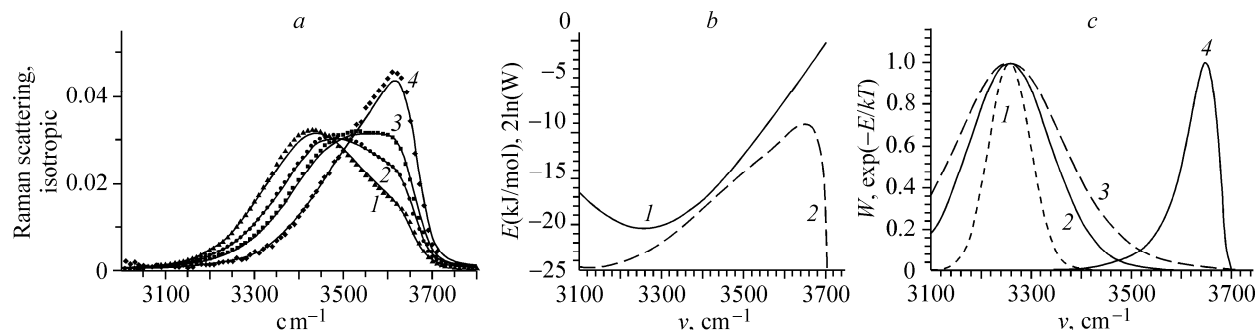


**Fig. 1.** (a) Experimental spectra (points) and OH vibration spectra of liquid water at constant density reconstructed [11] by (1) (solid curves) in the isotropic component of Raman scattering,  $T = 0^\circ\text{C}$ ,  $50^\circ\text{C}$ ,  $90^\circ\text{C}$ ,  $200^\circ\text{C}$  (from left to right); (b) frequency dependence of the  $E(\nu)$  (curve 1) and doubled logarithm  $W(\nu)$  functions (curve 2) of (1) calculated [21] from the IR spectra of water in the range  $10\text{-}200^\circ\text{C}$ ; the form of the statistical integral  $Q(T)$  is also found in [21]; (c) factors of Eq. (1):  $W(\nu)$  (curve 4) and Boltzmann's exponential  $\exp[-E(\nu)/(k_B T)]$  for  $T = -200^\circ\text{C}$  (curve 1),  $0^\circ\text{C}$  (2),  $200^\circ\text{C}$  (3).

function  $W(\nu)$  (curve 4) and the Gaussian-like Boltzmann's exponential  $\exp[-E(\nu)/(k_B T)]$ , monotonously broadening at elevated temperatures (curves 1-3). It is interesting to note that all extraordinary temperature transformations of the experimental spectra (Fig. 1a) are determined by the region of the overlap of the far wings of the two functions shown in Fig. 1c.

Regrettably, formula (1) is essentially phenomenological. It does not contain any structural parameters; both the energy and the degeneracy of the configurations of the hydrogen bridge are directly related to the frequency  $\nu$ . In particular, all possible combinations of bond lengths and bending angles, ultimately giving the same energy  $E$ , contribute to the same frequency  $\nu(E)$ . The fraction of these possible configurations among the total number of configurations determines the degeneracy  $W(\nu)$ , which in principle should contain information about the diversity of H-bond configurations in water. Surprisingly, this simple hypothesis was justified with a high degree of accuracy. However, it was desirable to attempt to exceed the bounds of the phenomenological approach and examine the particular relationship between the geometrical parameters of the hydrogen bridge configuration and the corresponding  $\nu_{\text{OH}}$  frequency in the vibrational spectrum and hence with the H-bond energy. This can be done within the framework of spectroscopy by analyzing the  $W(\nu)$  function of (1).

Let us have the set of all geometrical parameters of the O-H...O fragment affecting the  $\nu$  frequency denoted by  $G$ , and the measure of the set of configurations that generate this frequency, by  $W(G)$ . For the area differential to be preserved in the configuration and frequency representations,  $W(G)dG$  should equal  $W(\nu)d\nu$ , or, in the integral representation,

$$\int_{G:\nu \leq \nu_{\text{OH}}} W(G)dG = \int_0^{\nu_{\text{OH}}} W(\nu)d\nu. \quad (2)$$

That is, the integral of the known function  $W(\nu)$  (Fig. 1) from zero to any value of  $\nu_{\text{OH}}$  specified in advance should equal the integral over the domain of the desired function  $W(G)$  that covers all sets of values of the geometrical parameters  $G$  corresponding to the frequencies  $\nu \leq \nu_{\text{OH}}$ . If the set  $G$  contains several geometrical parameters, integral equation (2) generally leads to an incorrect inverse problem, whose solution requires special approaches. In this work, we consider the simplest cases when the H-bond energy depends on only one geometrical parameter and an unambiguous solution is possible. These cases include two widely known explanations to the anomalous broadening of the spectral bands of water, namely, the dependence of the  $\nu_{\text{OH}}$  frequency on the length  $R_{\text{O...O}}$  of the H-bond [22, 23] and on its bending angle  $\varphi(\text{H-O...O})$  [24, 25], respectively. In recent works [16, 18, 20], variation of the hydrogen bond lengths was again stated to be the major reason for the difference between the OH-oscillator frequencies of the water molecules.

The geometry of the O-H...O hydrogen bridge is generally defined in terms of the bond length  $R = R_{\text{O...O}}$  and the bending angle (deviation from the linear H-bond)  $\varphi = \varphi(\text{H-O...O})$ . Then the pure geometrical (ignoring energy) probability for the proton-donor  $\text{H}_2\text{O}$  molecule to meet the oxygen atom belonging to the proton-acceptor molecule in a liquid and lying

at a distance  $R \pm dR/2$  and at an angle  $\varphi \pm d\varphi/2$  relative to the direction of the O–H group is defined in terms of the differential of the conical section of the sphere layer,

$$W(R, \varphi) dR d\varphi = 4\pi R^2 \sin(\varphi) dR d\varphi. \quad (3)$$

For a hydrogen bond with this configuration, the role of energy is reflected in the total probability of realization of  $P(R, \varphi, T)$ , which is similar to (1), by the exponential  $\exp[-E(R, \varphi)/k_B T]$ . Thus, in the one-parameter representation of the hydrogen bond potential, we seek the dependences  $E(R)$  or  $E(\varphi)$ , respectively, that satisfy Eq. (1), that is, the dependences that describe, in terms of (1), the form and temperature evolution of the experimental spectra (Fig. 1a).

## RADIAL DEPENDENCE

Suppose the  $\nu_{OH}$  frequency is unambiguously defined in terms of the hydrogen bridge length  $R_{O\dots O}$  alone. A dependence of this kind,

$$\nu_{OH}(\text{cm}^{-1}) = 3707 - 2.222 \cdot 10^7 \cdot \exp(-3.925R), \quad R(\text{\AA}), \quad (4)$$

has long been known for crystals [27, 28], in which, because of the identity of all H-bonds of this type, the spectral lines are narrow enough and their frequencies can easily be compared to the corresponding crystallographic distances  $R_{O\dots O}$ . Formulas (2) and (3) allow us to find the analogous dependence for liquid for describing the temperature transformation of the experimental spectra. Since this variant ignored the effect of the  $\varphi$  angle, from (3) it follows that  $W(R) \sim R^2$ . Then (2) is recorded in a specific form as

$$J(\nu_{OH}) \equiv \int_{\nu_{\min}}^{\nu_{OH}} W(\nu) d\nu = \int_{R_{\min}}^{R_{O\dots O}} W(R) dR = (R_{O\dots O}^3 - R_{\min}^3) / (R_{\lim}^3 - R_{\min}^3). \quad (5)$$

Here  $R_{\min}$  is the minimum distance between water molecules in a liquid, and  $\nu_{\min}$  is the OH vibration frequency at  $3100 \text{ cm}^{-1}$  corresponding to this close contact of molecules, from which the statistical distribution  $P(\nu_{OH})$  starts [11]. Then from (4) it follows that  $R_{\min} = 2.677 \text{ \AA}$ . The third parameter in (5),  $R_{\lim}$ , is the limiting intermolecular distance  $R_{O\dots O}$  at which the O–H...O hydrogen bond in the given molecular pair still exists (the conventional estimate is  $\sim 3.3 \text{ \AA}$  [26]). The physical sense of the limiting length of the H-bond for liquid water is probably the fact that, in dense liquids, the exceedingly recessive partner is immediately replaced by a neighbor (which is now involved in the bond). The denominator from the right part of (5) plays the role of the normalizing factor that transforms it to unity for the limiting value of  $\nu_{OH} = \nu_u = 3707 \text{ cm}^{-1}$  (the vibration frequency of a free OH group) in the left part of the equation. The integral  $J(\nu_{OH})$  calculated from the  $W(\nu)$  function [21] is shown in Fig. 2. It is the basis for further calculations.

The solution of (5),

$$R_{O\dots O}(\nu_{OH}) = [R_{\lim}^3 + (R_{\lim}^3 - R_{\min}^3) J(\nu_{OH})]^{1/3}, \quad (6)$$

defines the relationship between  $R_{O\dots O}$  and  $\nu_{OH}$  (curve 1, Fig. 3a), that satisfies formula (1) after the  $E(\nu)$  function was recalculated, using (6), into  $E(R_{O\dots O})$ . Since this is an exact solution,  $E(R)$  (Fig. 3b, curve 1), together with  $W(R) = 4\pi R^2$ , automatically defines the shape of the experimental spectra and their temperature dependence shown in Fig. 1a. However, this  $\nu(R)$  dependence differs very strongly from the correlation curve  $\nu_{OH}(R_{O\dots O})$  known for crystals (curve 2, Fig. 3a, formula (4)). In addition, the  $E(R)$  dependence that follows from (6) (Fig. 3b, curve 1) is obviously unrealistic; it has a very narrow minimum at  $R = 2.678 \text{ \AA}$ , which is almost indiscernible on the scale of Fig. 3b. (Note that a minimum on the  $E(\nu)$  curve is an essential condition of a correct description of the low-frequency wing of the spectra at low temperatures [11].) The consequence of this is absolutely nonphysical behavior of the calculated distribution of the hydrogen bond lengths  $P(R, T)$ ,

$$P(R_{O\dots O}, T) = Q^{-1}(T) W(R_{O\dots O}) \exp[-E(R_{O\dots O}) / (k_B T)] \quad (7)$$

with narrow maxima near  $R_{\min}$ , which are not given here.

At first sight, the inadequacy of the one-parameter  $E(R)$  dependence is evidently the reason for the discrepancy between the calculation and experiment. It is not excluded, however, that the reason is the  $W(R)$  dependence which was adopted a priori and is valid for an arbitrary distribution in the space of points but not finite-sized objects. As can be seen

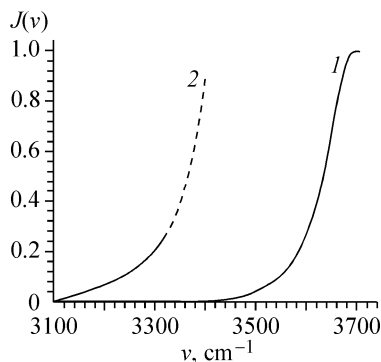


**Fig. 2.** Basis for further calculations: the left part of (5)  $J(v_{\text{OH}})$  as the antiderivative of the  $W(v)$  function (the function of the upper limit of integration). The left curve (2) is multiplied by 150 and demonstrates the behavior of  $J(v_{\text{OH}})$  at low frequencies.

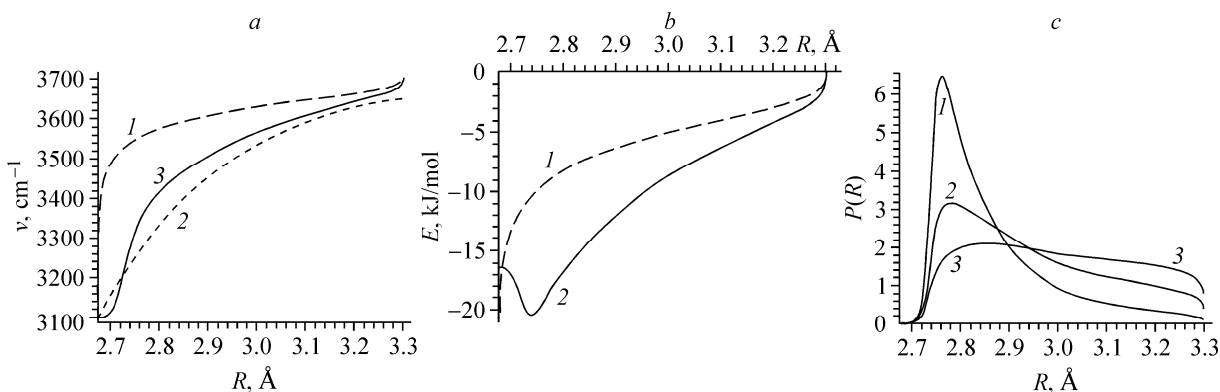


**Fig. 3.** (a) Dependence of the OH vibration frequency on the length of the hydrogen bridge according to formula (6) (curve 1); empirical correlation by formula (4) [28] (curve 2); as calculated from  $J(v_{\text{OH}})$  (Fig. 2) for  $W(R) = 4\pi(R - R_{\text{min}})^2$  (curve 3); (b) dependence of the H-bond energy on the length of the hydrogen bridge  $R_{\text{O}\dots\text{O}}$  calculated from  $E(v)$  in Fig. 1b using (6) for  $W(R) = 4\pi R^2$  (curve 1) and for  $W(R) = 4\pi(R - R_{\text{min}})^2$  (curve 2); (c) temperature dependence of the distribution of the lengths of the hydrogen bonds in water calculated from  $E(R)$  (curve 2, Fig. 3b) for  $W(R) = 4\pi(R - R_{\text{min}})^2$ ;  $T = 0^\circ\text{C}, 100^\circ\text{C}, 200^\circ\text{C}$  (from top to bottom).

from Fig. 1b, the  $W(v)$  function starts almost from zero (at  $v = v_{\text{min}}$ ) and changes in its domain by four orders of magnitude, whereas  $W(R) = 4\pi R^2$  on its left ( $R = R_{\text{min}}$ ) and right ( $R = R_{\text{lim}}$ ) boundaries differ only 1.5-fold. As a result, the  $v(R)$  dependence obtained by (5) transforms the very wide frequency range between  $3100 \text{ cm}^{-1}$  and  $3500 \text{ cm}^{-1}$  in the spectrum into minor surroundings of the  $R_{\text{O}\dots\text{O}}$  distances near  $2.7 \text{ \AA}$  (curve 1, Fig. 3a). Therefore, the distribution of intermolecular distances calculated by (7) differs widely from the first maximum on the experimental RDFs of liquid water [29] and in computer simulation [26], where it is much wider and centered to the right of  $R_{\text{O}\dots\text{O}} = 2.85 \text{ \AA}$ .

A palliative solution could be the dependence

$$\begin{aligned} W(R) &= 0, R \leq R_{\text{min}} \\ 4\pi(R - R_{\text{min}})^2, R > R_{\text{min}}, \end{aligned} \quad (8)$$

which limits the intermolecular distance to the hard sphere radius and starts from zero. Then the  $v(R)$  dependence calculated from the left part of (5) (curve 3, Fig. 3a) approaches empirical correlation (4) (curve 2, Fig. 3a), and the minimum of the potential well  $E(R)$  is shifted to  $2.75 \text{ \AA}$  (curve 2, Fig. 3b), which almost coincides with the equilibrium H-bond length in Ih

ice. The distribution of the hydrogen bond lengths  $P(R, T)$  calculated by (7) for this situation (Fig. 3c) is now not so substantially different from the first maximum of the RDF of water, its temperature behavior included [29].

## ANGULAR DEPENDENCE

Let us now have the  $\nu_{\text{OH}}$  frequency determined by the bending angle  $\varphi(\text{H-O}\dots\text{O})$  [24, 25], but not by the length  $R_{\text{O}\dots\text{O}}$  of the hydrogen bridge. Then according to (3),  $W(\varphi) \sim \sin(\varphi)$ , and (2) is reduced to

$$J(\nu_{\text{OH}}) \equiv \int_{\nu_{\text{min}}}^{\nu_{\text{OH}}} W(\nu) d\nu = \int_0^{\varphi(\nu_{\text{OH}})} W(\varphi) d\varphi = \{1 - \cos[\varphi(\nu_{\text{OH}})]\} / [1 - \cos(\varphi_{\text{lim}})]. \quad (9)$$

Here the measure of a set of angles with the given  $\varphi$  value is the length of a circle that forms a cone with a  $\varphi$  angle, and the limiting angle  $\varphi_{\text{lim}}$ , the angle of cleavage (switch-over) of the hydrogen bond, has the same sense as  $R_{\text{lim}}$  in (5). As a result, the desired dependence of the  $\nu_{\text{OH}}$  frequency on the  $\varphi$  angle, as well as the dependence on the  $R$  bond length in (5), is expressed in terms of the antiderivative of  $W(\nu)$ , i.e., in terms of  $J(\nu_{\text{OH}})$ ,

$$\varphi(\nu_{\text{OH}}) = \arccos\{1 - [1 - \cos(\varphi_{\text{lim}})]J(\nu_{\text{OH}})\} \quad (10)$$

and is shown in Fig. 4a. (For simplicity, the limiting angle  $\varphi_{\text{lim}}$  is set equal to  $\pi/2$ , which affects only the scale of the angle axis.) The dependence of the hydrogen bond energy on the bending angle  $E(\varphi)$  derived from  $E(\nu)$  (Fig. 1b) using (10) is shown in Fig. 4b, and the calculated angle distributions

$$P(\varphi, T) = Q^{-1}(T)\sin(\varphi)\exp[-E(\varphi)/(k_{\text{B}}T)] \quad (11)$$

at three temperatures are depicted in Fig. 4c. As in the case of the radial dependence, they differ substantially from the known distributions [26, 30]. The maxima of the distributions calculated for different temperatures are shifted toward small angles, and the shift values are approximately two- or threefold compared with the literature data; the half-widths are two or three times smaller. Unfortunately, we did not find the results of direct experimental measurements of these distributions.

The minimum of the  $E(\varphi)$  curve near  $5^\circ$  is (formally) a consequence of the same minimum on the  $E(\nu)$  curve in Fig. 1b. In terms of the single significant parameter (angle), the optimum character of the slightly bent hydrogen bond could be explained by the steric factor of interaction between two H-bonds formed by the OH groups of one molecule, as is the case with, e.g., ices. Recall that the numerical value of  $\varphi_{\text{lim}}$  in (9) and (10) affects only the scale of the abscissa axis and was chosen randomly. In particular, replacement of  $\varphi_{\text{lim}} = 90^\circ$ , for example, by  $45^\circ$  will only lead to the curves “extended” twofold in Fig. 4; it suffices to replace  $90^\circ$  by  $45^\circ$  on the corresponding axis. Incidentally, this improves agreement with the data of [26, 30] for the position and width of the calculated distributions of angles, although the shapes and temperature dependences are still different.

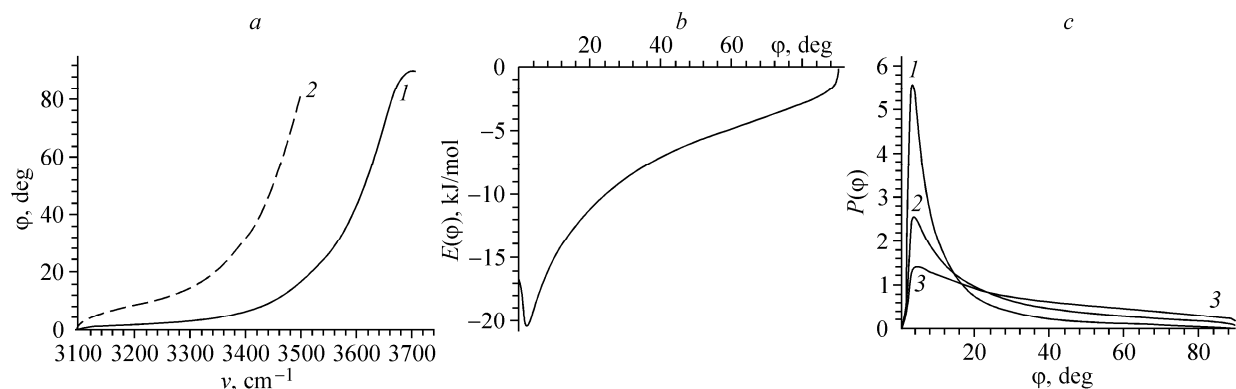


**Fig. 4.** (a) Relationship between the  $\varphi(\text{H-O}\dots\text{O})$  bending angle of the hydrogen bond and the  $\nu_{\text{OH}}$  frequency that follows from (10) and allows a description of the transformation of the vibrational spectra as good as description by formula (1) (Fig. 1a); (b) dependence of the hydrogen bond energy  $E(\varphi)$  on the bending angle; (c) distributions of the bending angles of H-bonds in water calculated by formula (11);  $T = 0^\circ\text{C}$  (curve 1),  $100^\circ\text{C}$  (2), and  $200^\circ\text{C}$  (3).



## CONSTRUCTION OF ONE-PARAMETER POTENTIALS FROM EMPIRICAL CORRELATIONS

At first sight, the results of this study unambiguously indicate that one geometrical parameter is insufficient for describing the hydrogen bond potential. However, it is still doubtful whether or not the pure geometrical formulas (3) or (8), completely ignoring the specifics of the water structure, are too arbitrary assumptions. Isn't it better to proceed from the known empirical correlations of the  $\nu_{\text{OH}}$  frequency with the hydrogen bridge geometry and calculate the  $\{W(R), E(R)\}$  or  $\{W(\varphi), E(\varphi)\}$  functions from the previously obtained  $\{W(\nu), E(\nu)\}$  functions using these correlation dependences? We still consider this possibility, although  $W(\nu)$ , by definition, is a measure of *possible* states with the given frequency (and thus coincides with the distribution of the realized frequencies  $P(\nu)$  only at an infinite temperature, when the H-bond energy does not affect the probability of its realization [11]) and the structure is determined by the form of the potential. This approach is much simpler and does not require solving integral equation (2) and calculating the  $J(\nu_{\text{OH}})$  function.

Regretfully, we did not find in the literature a reliable empirical formula for the relationship between the frequency and the bending angle of the hydrogen bond similar to (4). Therefore, here we restrict our treatment to the case of the pure radial dependence of the hydrogen bond potential. Suppose that the relationship between  $R_{\text{O}\dots\text{O}}$  and  $\nu_{\text{OH}}$  is expressed, as in crystals, by correlation formula (4) (curve 2, Fig. 3a). Then replacing the  $\nu_{\text{OH}}$  frequency in equations for  $E(\nu)$  and  $W(\nu)$  by (4) and taking into account that

$$W(R) = W(\nu) |d\nu/dR|, \quad (12)$$

we can rerecord all formulas in terms of the  $R_{\text{O}\dots\text{O}}$  intermolecular distances. As in previous sections, we automatically obtain a description of the temperature evolution of the spectra (Fig. 1a) because of the conformity of the transformation.

The resulting  $W(R)$  and  $E(R)$  functions are shown in Fig. 5a and b, and the temperature evolution of the distribution of the hydrogen bond lengths is found in Fig. 5c. These distributions are much closer in shape and behavior to the first maximum of the experimental RDFs of water [29] than the distributions obtained in the "Radial Dependence" Section. It is interesting to note that the left wing of the  $W(R)$  dependence calculated by (12) and (4) is rather close to the parabola  $4\pi(R - R_{\text{min}})^2$  (Fig. 5a, curve 2), which we intuitively used above. Here  $R_{\text{min}} = 2.677 \text{ \AA}$ , which, by formula, (4) corresponds to the start of the frequency distribution in the spectrum,  $3100 \text{ cm}^{-1}$ . It is also interesting that the integral under this growing function is unity if  $R_{\text{lim}} = 3.2975 \text{ \AA}$ , which coincides with the conventional estimate,  $3.3 \text{ \AA}$  [1, 26]. This probably suggests that formula (8) adequately corrects the radial factor of (3) and includes the finite radius of atoms.

The presence of a maximum on the  $W(R)$  function is somewhat unexpected (curve 1, Fig. 5a). It is formally a consequence of the maximum on the  $W(\nu)$  function (Fig. 1c) and the monotonous  $\nu(R)$  dependence (formula (4)). Within the framework of this approach, termination of the unrestricted growth of  $W(R)$  can be explained by the fact that at distances of

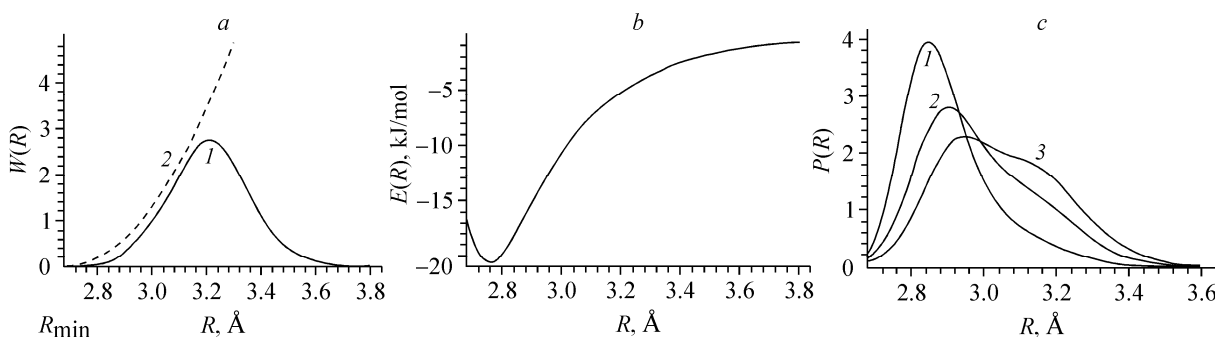


**Fig. 5.** (a) Solid curve 1:  $W(R)$  obtained from  $W(\nu)$  (Fig. 1b, c) by formula (4); dashed curve 2: segment of the curve  $W(R) = 4\pi(R - R_{\text{min}})^2$  equal in area; (b) dependence of the hydrogen bond energy on its length recalculated from Fig. 1b using formula (4); (c) hydrogen bond length distributions  $P(R, T)$  for  $T = 0^\circ\text{C}$  (curve 1),  $100^\circ\text{C}$  (2), and  $200^\circ\text{C}$  (3).

$\sim 3.1$  Å, the “unfavorable” partner is replaced by another partner lying more closely, and the hydrogen bond is switched over to the latter. As can be seen from Fig. 5, it is impossible to remain faithful to the former partner at distances longer than 3.5 Å from it. In the absence of competition, formula (8) would be valid. The switch-over of the hydrogen bond with replacement of the “unfavorable” counterpart is evidently absent in alcohols. In view of the bulky hydrophobic “tails,” when the partners are far away from each other at elevated temperatures, the existing hydrogen bond undergoes cleavage, but a new bond is not formed; this leads to a separate narrow line of the vibrations of the free OH group in the spectrum. The transformation of the wide high-frequency “shoulder” of the weak hydrogen bonds of water into a narrow line of the alcohol “monomers” is a very striking distinction in the temperature behavior of the spectra of these liquids [31].

## CONCLUSIONS

Our calculations showed that both literature alternative hypotheses about the reasons for the anomalously large broadening of the spectra of liquid water can formally allow us to describe the frequency distributions in experimental spectra over the whole accessible range of temperatures. However, the required  $\nu(R_{O\dots O})$  and  $\nu(\varphi)$  dependences disagree with the known empirical correlations between the corresponding quantities, and the distributions of the intermolecular distances  $P(R_{O\dots O})$  and angles  $P(\varphi)$  calculated from them are very different from the results of computer simulations and experimental RDFs of water. On the contrary, using the empirical correlation of  $\nu(R)$  as a basis allows us to achieve better agreement of the distribution function of the nearest neighbors with X-ray analysis data. However, the obtained behavior of the  $W(R)$  function demands a more adequate explanation and can hardly be described based on the first principle approach.

To summarize, the given approach is recommended for constructing more complex potentials including simultaneously all geometrical parameters of the hydrogen bridge that affect the H-bond energy. Using empirical correlation (4) could help us find a correct solution to the many-parameter integral equation (2) by seeking an angular dependence compatible with the behavior of the  $J(\nu_{OH})$  integral, providing agreement of the desired relation between the frequency and the geometrical parameters of the hydrogen bridge with the form and thermal behavior of the experimental spectra.

It is necessary to emphasize once again that this work deals with the potential of the hydrogen bond, that is, with the dependence of its energy on the distance between the molecules of the bond and their mutual orientation. This potential might be very useful, for example, for analyzing the already constructed computer models of water in order to reveal hydrogen bonds in them and construct the nets of these bonds, and for qualitatively describing the local properties and performing topology studies of the nets in general. With this approach one can readily calculate the vibrational spectrum for each model, independently testing the adequacy of the potentials of intermolecular interactions used for modeling to experiment. At the same time, this potential is evidently inapplicable for direct use in molecular dynamic or Monte Carlo calculations; it must be complemented with interactions that were ignored, primarily, mutual repulsion of bond partners and their interactions with other molecules.

The author is grateful to Yu. I. Naberukhin, N. N. Medvedev, and V. P. Voloshin for numerous discussions and useful comments. This work was supported by the Russian Foundation for Basic Research, grant Nos. 04-03-32560 and 07-03-00503-a.

## REFERENCES

1. G. G. Malenkov, *J. Struct. Chem.*, **47**, Supplem., 1-31 (2006).
2. W. C. Röntgen, *Ann. Phys. Chem. N.F.*, **XLV**, 91-97 (1891).
3. G. E. Walrafen, *J. Chem. Phys.*, **48**, 244-251 (1968).
4. A. P. Luck, in: *Structure of Water and Aqueous Solutions*, Verlag Chemie/Physik Verlag, Marburg (1974), pp. 221-284.
5. J. D. Bernal and R. H. Fowler, *J. Chem. Phys.*, **1**, 515-548 (1933).
6. Yu. I. Naberukhin, *Structural Models of Liquids* [in Russian], Novosibirsk State University (1983).



7. Yu. Ya. Efimov and Yu. I. Naberukhin, *Faraday Discuss. Chem. Soc.*, **85**, 117-123 (1988).
8. *Breakthrough of the Year*, *Science*, **306**, 2017 (2004).
9. Ph. Wernet, D. Nordlund, U. Bergmann, et. al., *ibid.*, **304**, 995-999 (2004).
10. Yu. Ya. Efimov and Yu. I. Naberukhin, *Faraday Discuss. Chem. Soc.*, **85**, 117-123 (1988).
11. Yu. Ya. Efimov and Yu. I. Naberukhin, *Mol. Phys.*, **101**, 459-468 (2003).
12. H. Palamarev and G. Georgiev, *Vibr. Spectr.*, **7**, 255-264 (1994).
13. Yu. Ya. Efimov and Yu. I. Naberukhin, *Mol. Phys.*, **102**, 1407-1414 (2004).
14. Yu. Ya. Efimov and Yu. I. Naberukhin, *Spectrochim. Acta A*, **61/8**, 1789-1794 (2005).
15. S. A. Corcelli and J. L. Skinner, *J. Phys. Chem. A*, **109**, 6154-6165 (2005).
16. H. Torii, *ibid.*, **110**, 9469-9477 (2006).
17. R. Kubo, *Adv. Chem. Phys.*, **15**, 101-127 (1969).
18. J. D. Smith, Ch. D. Cappa, K. R. Wilson, et. al., *Proc. Natl. Acad. Sci. USA*, **102**, 14171-14174 (2005).
19. A. P. Zhukovskii, *Zh. Strukt. Khim.*, **17**, 931/932 (1976).
20. C. P. Lawrence and J. L. Skinner, *J. Chem. Phys.*, **118/1**, 264-272 (2003).
21. Yu. Ya. Efimov and Yu. I. Naberukhin, *J. Struct. Chem.*, **41**, No. 3, 433-439 (2000).
22. M. I. Batuev, *Izv. Akad. Nauk SSSR, Ser. Fiz.*, **11(4)**, 336-339 (1947).
23. T. T. Wall and D. F. Hornig, *J. Chem. Phys.*, **43**, 2079-2087 (1965).
24. J. A. Pople, *Proc. R. Soc.*, **A205**, 163-178 (1951).
25. A. P. Zhukovskii, L. V. Shurupova, and M. A. Zhukovskii, *J. Struct. Chem.*, **36**, No. 3, 426-431 (1995).
26. G. G. Malenkov, "Structure of aqueous systems: models and numerical experiment," Chemical Sciences Doctoral Dissertation, Institute of Physical Chemistry, Moscow (1990).
27. M. Falk, *Chemistry and Physics of Aqueous Gas Solutions*, W. B. Adams et. al. (eds.), Electrochem. Soc. Inc., Princeton (1975), pp. 19-41.
28. Yu. Ya. Efimov, *J. Struct. Chem.*, **32**, No. 6, 834-841 (1991).
29. Yu. E. Gorbaty and Yu. N. Demianets, *Chem. Phys. Lett.*, **100/5**, 450-454 (1983).
30. K. Modig, G. Pfrommer, and B. Halle, *Phys. Rev. Lett.*, **90/7**, 075502(1-4) (2003).
31. Yu. Ya. Efimov and Yu. I. Naberukhin, *Zh. Strukt. Khim.*, **28**, No. 2, 88-92 (1981).